

# Effects of Coulomb interactions on the splitting of luminescence lines

Boris A. Rodriguez<sup>a</sup> and Augusto Gonzalez<sup>a,b</sup>

<sup>a</sup>*Instituto de Fisica, Universidad de Antioquia, AA 1226, Medellin, Colombia*

<sup>b</sup>*Instituto de Cibernetica, Matematica y Fisica, Calle E 309, Vedado, Ciudad Habana, Cuba.*

We study the splitting between the right-hand and left-hand circularly polarized luminescence lines in a quantum dot under relatively weak confinement regime and resonant high-power excitation. When the dot is populated with an even number of electron-hole pairs (biexciton and higher excitations), the splitting measures basically the Zeeman energy. However, in the odd number of pairs case, we have, in addition to the Zeeman and Overhauser shifts, a contribution to the splitting coming from Coulomb interactions. This contribution is of the order of a few meV, and shows distinct signatures of shell-filling in the quantum dot.

PACS numbers: 78.67.Hc, 71.70.Ej

Keywords: Quantum dots, Coulomb interactions, Zeeman splitting, Luminescence

## I. INTRODUCTION

This paper is aimed at a theoretical description of the splitting of luminescence lines coming from the deexcitation of a quantum dot in the presence of a magnetic field. There are a few factors contributing to this splitting.

First, there is a contribution coming from the Zeeman energy, which is proportional to the magnetic field,  $B$ . As luminescence lines arise from exciton recombination, both the electron and hole Lande factors enter the expression for the Zeeman shift. In a nanostructure, Lande factors exhibit a dependence not only on the semiconductor band structure, but also on the geometry. In the recent past, for example, extensive studies on the dependence on well width<sup>1</sup> have been conducted. For magnetic fields between 1 and 3 Teslas, the typical values we will encounter for the Zeeman shifts are 0.05 - 0.2 meV.

A second contribution to the splitting is the so called Overhauser shift<sup>2</sup>. It is originated in the hyperfine interaction between the electron and nuclear spins. The electron motion around the nanostructure induces a nuclear spin polarization. Once the nuclear polarization is set up, the interaction of the electron with the thousands of nuclei conforming the dot leads to a measurable shift in the luminescence lines. In a first approximation, the Overhauser shift does not depend on the magnetic field nor on the quantum dot size, but increases up to a saturation value with the excitation power. The latter fact can be understood in terms of the increase of the nuclear polarization as the rate of electron-hole pair creation is raised. Typical values of the Overhauser shift are around 0.1 meV. Recent measurements of this contribution were done on quantum dots formed from width fluctuations in a well<sup>3</sup>, and on self-assembled quantum dots<sup>4</sup>.

There is a third contribution to the splitting, which shall appear when the excitation power is high enough to create multiexcitonic complexes. Recombination of one electron-hole pair from a complex involves Coulomb interactions in a nontrivial way. The emission of a right-hand circularly polarized photon proves to be not equivalent to the emission of a left-hand circularly polarized one. Typical values for this shift are around 3 meV, i.e.,

the values of energy separations between electronic states in the complex. These Coulomb interaction effects have not been studied experimentally nor theoretically so far. They constitute the focus of our attention.

The plan of the paper is as follows. In Sec. II, we present a brief resume of known ideas explaining the experimental results of Refs. [3,4], which correspond to low excitation power and independent exciton recombination. This section is intended as an introduction to Sec. III, where higher excitations are considered. Multiexcitonic complexes are treated in the framework of a corrected BCS scheme, which takes a proper account of mean field Coulomb interactions and Fermi statistics. We compute the position and intensities of luminescence lines coming from the decay of systems with up to 21 pairs. The main results are the absence of Overhauser or Coulomb interaction effects in complexes with an even number of pairs, and the shell filling effects in the shifts due to Coulomb interactions for systems with an odd number of pairs. Concluding remarks are given in the last section.

## II. THE INDEPENDENT-EXCITON APPROXIMATION TO THE $\sigma_+$ - $\sigma_-$ SPLITTING

The experiments<sup>3,4,5</sup> are usually performed in the so called Faraday configuration, where the excitation laser beam is parallel to the applied magnetic field, and backscattering geometry. A schematic view is presented in Fig. 1.

The model parameters are chosen to fit (at least qualitatively) the experimental setup described in paper [5]. A quasi twodimensional quantum dot is formed from width fluctuations in a 4.2 nm-wide GaAs-AlGaAs quantum well. The dot area is around  $10^3$  nm<sup>2</sup>. Taking into account that the GaAs lattice constant is  $\sim .3$  nm, the number of nuclei in the dot is  $\sim 10^5$ .

A simplified two-band structure for GaAs is assumed. A schematics of the band structure is drawn in Fig. 2, where electron - hole coupling for each light polarization, and Zeeman splitting in each sub-band are indicated. The effective electron and heavy-hole Lande fac-

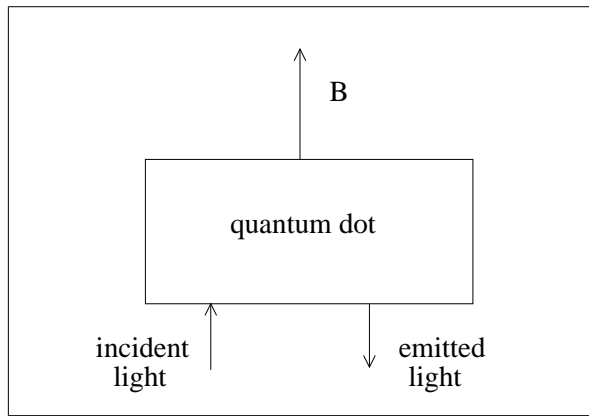


FIG. 1: Geometry of the experiment.

tors for the 4.2 nm-wide quantum well are expected to be  $g_e \approx 0.1$ ,  $g_h \approx -1.2$ .<sup>1</sup> The Zeeman energy of an electron-hole pair is computed from:

$$\varepsilon_{Zeeman} = \mu_B B(g_e S_e - g_h S_h) = \mu_B B(g_e + g_h) S_e, \quad (1)$$

where  $\mu_B = 0.057$  meV/Teslas is the atomic Bohr magneton, and  $S_e, S_h = \pm 1/2$  are the electron and hole spin projections over  $B$ , which acts along the dot normal.  $g_e + g_h \approx -1.1$  is the exciton Lande factor.

The quantum dot is resonantly excited, i.e., the laser excitation energy is only a few meV above the luminescence lines. Consequently, in luminescence there is memory of how the dot is pumped. Notice that the sense of rotation of the electric field is inverted for the emitted light. This means that by pumping with  $\sigma_+$  light, for example, we are in fact populating the  $\sigma_-$  mode for backward emission.

As mentioned before, there are around  $10^5$  nuclei in our GaAs dot. Half of them are  $^{69}\text{Ga}$  and  $^{71}\text{Ga}$  nuclei with relative abundances 60% and 40% respectively. The second half corresponds to  $^{75}\text{As}$  nuclei. For all these nuclei, the total spin is  $I = 3/2$ . Their magnetic moments (in units of the nuclear magneton,  $\mu_n$ ) are, respectively, 2.017, 2.562 and 1.439.<sup>6</sup>

The hyperfine interaction between one conduction band electron and nuclei in the quantum dot is described by the Hamiltonian:

$$\mathcal{H}_{en} = \alpha \sum_n \vec{S}_e \cdot \vec{I}_n |\psi_e(\vec{r}_n)|^2, \quad (2)$$

where  $\alpha = (2/3)\mu_0 g_e g_n \mu_B \mu_n$ , and  $\mu_0$  is the magnetic permittivity of vacuum.  $\psi_e$  is the electron wave function, which contains both an envelope (orbital) part and the Bloch functions, which are  $s$ -functions.  $\psi_e$  is evaluated at the positions of the nuclei, i.e. the origin of each cell. For Bloch  $s$ -functions,  $\phi$ , we have  $|\phi(0)|^2 \approx Z^3/(a_B n)^3$ , where  $Z$  is the atomic number (31 for Ga and 33 for As),

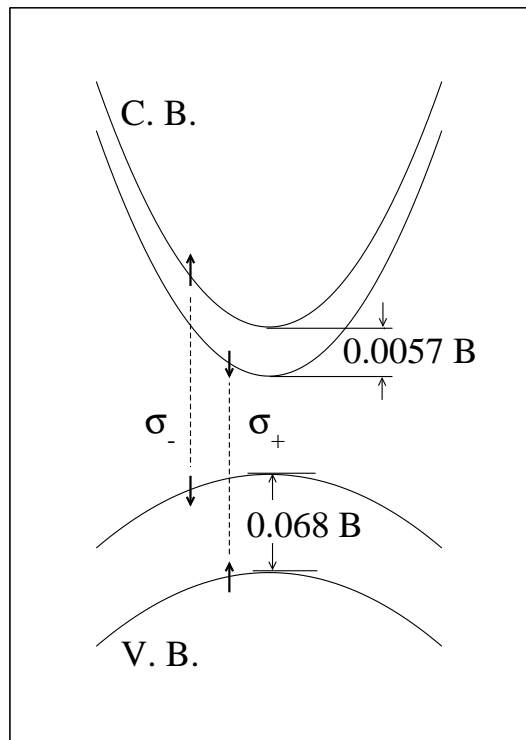


FIG. 2: Schematics of the assumed band structure in the dot. The electron-hole pairs created in the absorption of  $\sigma_+$  and  $\sigma_-$  photons are drawn.

$a_B$  is the Bohr radius, and  $n = 4$  corresponds to the 4s electrons conforming the conduction band. The fact that the orbital wave function is extended all over the dot (meaning that the square of the orbital wave function is proportional to  $1/N_n$ , where  $N_n$  is the number of nuclei in the dot) make the hyperfine contribution to the energy, Eq. (2), roughly independent of the dot size. In a mean field approximation,  $\langle \vec{I} \rangle$  is oriented along  $B$ , and we get for the interaction energy of one electron with the  $10^5$  nuclei in the dot:

$$\varepsilon_{hyperfine} = g_{en} \langle I \rangle S_e. \quad (3)$$

The  $g_{en}$  constant for bulk GaAs was found to be around -0.090 meV.<sup>7</sup> A similar value was observed in the quantum dots studied in Refs. 5 and 3.

Finally, there is a contribution to the exciton energy coming from the electron-hole exchange interaction in a deformed quantum dot. For the quantum dot under study<sup>8</sup>, we have

$$\varepsilon_{\pm}^{(exch)} \approx \mp 0.012 \text{ meV}. \quad (4)$$

With the help of Eqs. (1,3,4), and the independent exciton approximation, we write the single pair energy in the form:

$$\varepsilon_{\pm} = \varepsilon_X + \varepsilon_{\pm}^{(exch)} + \mu_B B(g_e + g_h)S_e + g_{en}\langle I \rangle S_e, \quad (5)$$

where the + index corresponds to  $S_e = 1/2$  ( $\sigma_+$  polarization of the emitted light), and the - index to  $S_e = -1/2$  ( $\sigma_-$  polarization of the emitted light).  $\varepsilon_X$  is the contribution of the electron-hole Coulomb attraction.  $\varepsilon_{\pm}$  gives, respectively, the position of the  $\sigma_+$  and  $\sigma_-$  luminescence lines. The shift between them is

$$\Delta\varepsilon = \varepsilon_- - \varepsilon_+ = \varepsilon^{(exch)} - \mu_B B(g_e + g_h) - g_{en}\langle I \rangle. \quad (6)$$

It depends on the excitonic populations,  $N_+$ ,  $N_-$ , through  $\langle I \rangle$ . The Overhauser shift is, by definition,

$$\Delta\varepsilon_{Overhauser} = -g_{en}\langle I \rangle. \quad (7)$$

It can be measured by turning off the contribution of each nuclear species to the mean nuclear spin with the help of microwave radiation sintonized to the frequency of the corresponding nuclear magnetic resonance<sup>9</sup>. Under  $\sigma_+$  pumping, the electron spin polarization is  $\langle S_e \rangle < 0$ , and the mean nuclear spin is  $\langle I \rangle > 0$  in order to minimize the hyperfine interaction energy. This means that the Overhauser shift is added to the Zeeman splitting. Under  $\sigma_-$  pumping, on the contrary, the Overhauser shift is subtracted from the Zeeman splitting.

### III. ACCOUNT OF MANY-PARTICLE COULOMB INTERACTIONS

In the independent-exciton approximation, Eq. (5), the dependence on pumping comes only from  $\langle I \rangle$ . In the experiments reported in Refs. 3,4, the mean exciton number in the dot is less than one. In paper 5, there is a study of the dependence of  $\Delta\varepsilon$  on the excitation power, but what is indeed observed in the single-exciton line is the saturation of the nuclear polarization,  $\langle I \rangle$ , as the occupation of the exciton state increases.

In the present section, we shall discuss the more general situation, where the excitation power is enough to create a few pairs in the dot. Many-body Coulomb interactions may introduce an additional dependence of  $\Delta\varepsilon$  on  $N_+$  and  $N_-$ . The energy of a system with  $N_+, N_-$  pairs is written as:

$$\begin{aligned} E(N_+, N_-) &= E_{Coul}(N_+, N_-) \\ &+ \mu_B B(g_e + g_h)(N_+ - N_-)/2 \\ &+ g_{en}\langle I \rangle(N_+ - N_-)/2, \end{aligned} \quad (8)$$

where  $E_{Coul}$  accounts for Coulomb interactions among particles. The positions of the  $\sigma_+$  and  $\sigma_-$  lines are obtained from:

$$\begin{aligned} \varepsilon_+ &= E_{Coul}(N_+, N_-) - E_{Coul}(N_+ - 1, N_-) \\ &+ \mu_B B(g_e + g_h)/2 + g_{en}\langle I \rangle/2, \end{aligned} \quad (9)$$

$$\begin{aligned} \varepsilon_- &= E_{Coul}(N_+, N_-) - E_{Coul}(N_+, N_- - 1) \\ &- \mu_B B(g_e + g_h)/2 - g_{en}\langle I \rangle/2. \end{aligned} \quad (10)$$

Coulomb interactions introduce a contribution to the shift:

$$\Delta\varepsilon_{Coul} = E_{Coul}(N_+ - 1, N_-) - E_{Coul}(N_+, N_- - 1). \quad (11)$$

It is reasonable to accept that  $E_{Coul}$  does not vary when  $N_+$  and  $N_-$  are interchanged:  $E_{Coul}(N_+, N_-) = E_{Coul}(N_-, N_+)$ .

In order to compute  $E_{Coul}$ , we use a model of parabolic dot with harmonic confinement,  $\hbar\omega \approx 10$  meV. This value of  $\omega$  is chosen to reproduce the exciton diamagnetic shift of 0.025 meV/Teslas<sup>2</sup> reported in Refs. [3,5]. The corresponding oscillator length is around 12 nm, a value similar to the dot characteristic dimensions. Effective masses  $m_e = 0.067 m_0$ ,  $m_h = 0.15 m_0$ , and relative dielectric constant  $\kappa = 12.5$  are used. Electron-hole pairing is accounted for by means of a BCS wave function. Notice that the Bohr radius for GaAs is around 7 nm. This means that the area occupied by an exciton is around 150 nm<sup>2</sup>. In our 10<sup>3</sup> nm<sup>2</sup> dot, 7 excitons are already closed packed, and the effects of Fermi statistics should be important. These effects and the mean field Coulomb interactions are correctly described by the BCS function.

Fluctuations in the particle number, not conserved by the BCS function, are important for a system with around 10 pairs. Thus, the BCS function should be projected onto a subspace with fixed particle number. The projection scheme we use is the so called Lipkin-Nogami scheme<sup>10,11</sup>. In the present situation, we shall use a Lipkin-Nogami scheme with two conserved charges,  $N_+$  and  $N_-$ . As this situation is not common in the literature, we give in the Appendix a brief description of the method and the explicit equations to be used.

Let us first discuss the simplest case beyond the independent exciton approximation: the  $\sigma_+ - \sigma_-$  splitting in the biexciton line.

The lowest biexciton state has  $(N_+, N_-) = (1, 1)$ . The first state with  $N_+$  or  $N_-$  equal to 2 has excitation energy higher than 8 meV (with our model parameters). Under quiresonant excitation and temperatures below 4 K, only the ground state will be populated with high probability.

The Coulomb contribution to the splitting, Eq. (11), is thus zero for the biexciton lines. It is not difficult to see that the Overhauser shift is also zero or, at least, much smaller than the shift for the exciton. Indeed, an intuitive argument suggests that, as the spin polarization is zero in the ground state, the mean nuclear spin will be zero too.

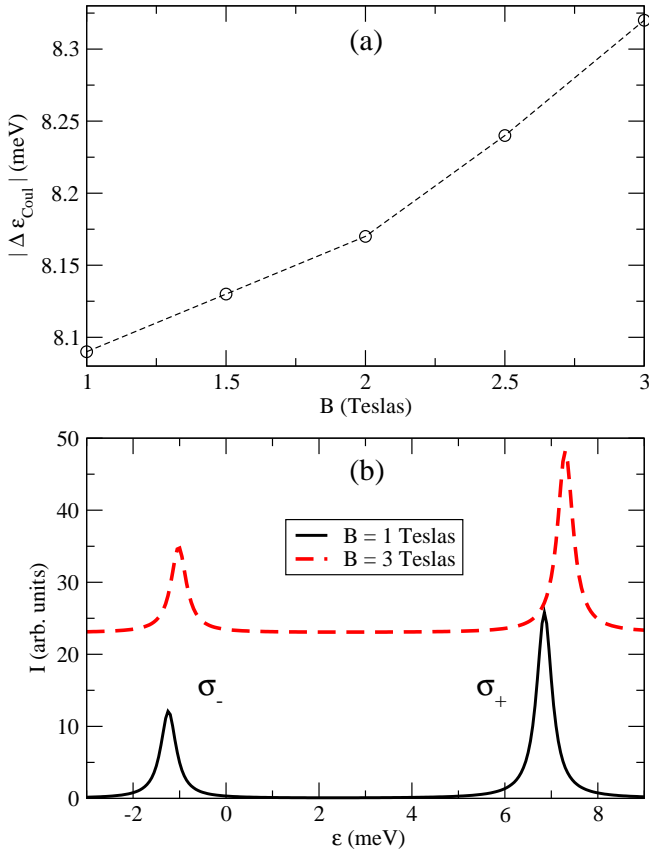


FIG. 3: (Color online) (a) Coulomb contribution to the  $\sigma_+ - \sigma_-$  splitting in the  $(N_+, N_-) = (2, 1)$  system, (b) Intensities of the luminescence lines at  $B = 1$  and 3 Teslas. The reference energy is  $E_{gap}$ . Only Coulomb interactions are included when computing the line positions.

In fact, the situation is a bit more complicated. One can guess that, as each excitation has a certain weight in the density matrix, exciton states, including the long-lived dark states, play an important role in determining the mean nuclear spin<sup>3</sup>. Nevertheless, a lower value for  $\langle I \rangle$  is expected and, consequently, a lower shift due to the Overhauser effect.

There is, nevertheless, a very important effect of Coulomb interactions consisting in the concentration of the luminescence in a single, coherent, line, as will become clear below.

The conclusion is that the biexciton lines exhibit a weakened Overhauser effect, and no shift coming from Coulomb interactions among particles. This conclusion can be extended to any states with  $N_+ = N_-$ , i.e., when there is an even number of pairs in the dot.

The situation is different, however, when the number of pairs is odd. Let us consider, for example, the  $(N_+, N_-) = (2, 1)$  case. We expect a nonzero mean nuclear polarization and, consequently, a nonzero Overhauser shift. The magnitude of this shift is expected to be around 0.1 meV. The Coulomb contribution to the

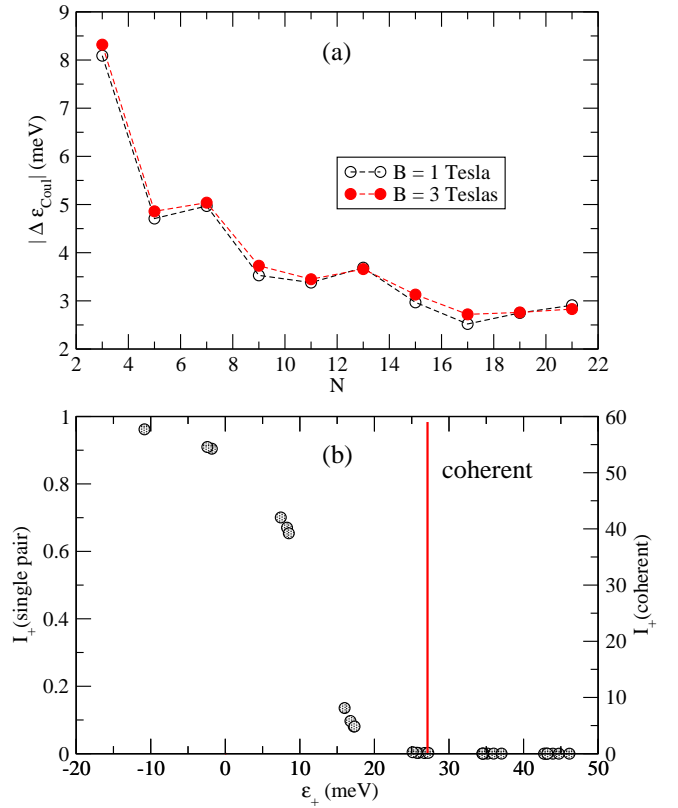


FIG. 4: (Color online) (a) Splitting induced by Coulomb interactions as a function of the number of pairs in the dot, (b) Comparison between single-pair and coherent  $\sigma_+$  luminescence in the  $(N_+, N_-) = (7, 6)$  system at  $B = 1$  Tesla.

splitting is much greater, of the order of a few meV.

We show in Fig. 3(a) the Coulomb splitting for the luminescence lines coming from the decay of the  $(2, 1)$  system as a function of the magnetic field,  $B$ . Notice the smooth dependence of  $\Delta\varepsilon_{Coul}$  on  $B$ . We shall stress that, when computing the position of the lines,  $\varepsilon_{\pm}$ , we assume transitions from the ground state of the  $(N_+, N_-)$  system to the ground states of the  $(N_+ - 1, N_-)$  and  $(N_+, N_- - 1)$  systems. We verified that these so called coherent luminescence lines account for more than 80 % of the total luminescence (see Appendix). We represent in Fig. 3(b) the relative intensities of both lines at  $B = 1$  and 3 Teslas. Only Coulomb interactions are included in the line positions. The reference energy is the band gap. Lorentzians with a width  $\Gamma = 0.2$  meV are used to represent the lines. The variation of the magnetic field induces a blueshift on both line positions, which is of 0.45 meV for the  $\sigma_+$  line, and 0.22 meV for the  $\sigma_-$  line. For comparison, let us notice that the Zeeman energy (not included in the figure) moves the  $\sigma_+$  line 0.062 meV to the left, and the  $\sigma_-$  line 0.062 meV to the right, when  $B$  varies from 1 to 3 Teslas.

The luminescence lines coming from the decay of the  $(2, 1)$  system shall be observed under  $\sigma_-$  excitation. Due

to the reasons mentioned above for the biexciton, the excitation of the (3,0) system is hardly possible. Under  $\sigma_+$  excitation,  $\Delta\varepsilon_{Coul}$  changes sign, and the lines interchange the intensities.

It is interesting to look at still higher excitations. To be definite, we consider  $\sigma_-$  pumping and follow only the luminescence lines coming from the decay of the  $(n+1, n)$  systems. The splitting induced by Coulomb interactions is drawn in Fig. 4(a) as a function of the total number of pairs,  $N = 2n + 1$ . The splitting is close to the harmonic confinement energy,  $\hbar\omega_0 = 10$  meV, for the  $N = 3$  system, but only around 3 meV for the  $N=21$  complex. We observe also distinct signatures of shell filling at the magic numbers  $N - 1 = 2, 6, 12$  and 20.

The effects of Coulomb interactions are made evident in Fig.4(b), where single-pair and coherent  $\sigma_+$  luminescence in the  $(N_+, N_-) = (7, 6)$  system at  $B = 1$  Tesla are compared. The single-pair luminescence is evaluated from the pair energies and occupations. We see the two main effects of Coulomb interactions in this figure. First, there is a strong enhancement of luminescence intensity. This is the analog of the well known exciton effect. Second, the coherent peak is shifted with respect to the position of the single-pair peaks.

Finally, we shall stress that, for a multiexciton system with  $N > 2$  to live in a quantum dot, the confining potential should correspond to a deep well, because these systems are, most likely, unbound<sup>12</sup>. This does not seem to be the situation reported in [5,3], where the dot is formed as a result of fluctuations in the well width. It does not represent, however, a limitation to the validity of our results, because quantum dots with the desired properties can presently be grown at will.

#### IV. CONCLUDING REMARKS

We have shown that luminescence lines arising from the decay of one electron-hole pair in a multiexcitonic complex may exhibit a strong asymmetry with respect to the sense of circular polarization of the emitted light if the number of pairs in the complex is odd. Let us stress the conditions under which this statement is expected to be valid.

First, it was assumed that  $N_+ - N_- = \pm 1$ . Luminescence lines from the complex with  $N_+ = N_-$  were shown to exhibit roughly no Overhauser nor Coulomb shifts. From an experimental point of view, a small disbalance between  $N_+$  and  $N_-$  is expected under quasidegenerate excitation and very low temperatures. High excitation powers are needed to create the multiexcitonic complexes.

A second, very important, assumption is the coherent (collective) character of the decay process. Lines which can be interpreted as single- or independent-pair decays are possible too. One can guess that these single-pair decays should play an important role in luminescence under a strong confinement regime and well above band gap excitation<sup>13</sup>. In our calculations, we assumed an inter-

mediate confinement regime,  $\hbar\omega_0 = 10$  meV, in which case effects due to Coulomb interactions become very important, and the coherent luminescence accounts for more than 80 % of the total luminescence. The effects of Coulomb interactions were shown to be basically the following: and enhancement of luminescence intensity and concentration on a single line, which is shifted with respect to the position of the single-pair decays. Band-filling in the quantum dot is seen as a blueshift of the peak position.

#### Acknowledgments

The authors acknowledge the Comitee for Research of the Universidad de Antioquia for support.

#### APPENDIX A: LIPKIN-NOGAMI SCHEME WITH TWO CONSERVED CHARGES

The Hamiltonian describing the electron-hole system in the two-dimensional quantum dot is written as:

$$\begin{aligned}
 H = & \sum_n \left( t_n^{(e)} e_n^\dagger e_n + t_n^{(h)} h_n^\dagger h_n \right) \\
 & + \frac{\beta}{2} \sum_{rsuv} \langle r, s | 1/r | u, v \rangle e_r^\dagger e_s^\dagger e_v e_u \\
 & + \frac{\beta'}{2} \sum_{rsuv} \langle r, s | 1/r | u, v \rangle h_r^\dagger h_s^\dagger h_v h_u \\
 & - \beta'' \sum_{rsuv} \langle r, s | 1/r | u, v \rangle e_r^\dagger h_s^\dagger h_v e_u, \quad (A1)
 \end{aligned}$$

where, for simplicity, we have not included electron-hole exchange terms.  $\beta = 0.8 e^2 / (4\pi\epsilon_0\kappa l_0)$  is the strength of electron-electron Coulomb interactions, whereas  $\beta'$  and  $\beta''$  characterize the hole-hole and electron-hole interactions. The calculations presented in the paper correspond to the symmetric situation, in which  $\beta = \beta' = \beta''$ . A factor of 0.8 is included in  $\beta$  to approximately account for the quasi two-dimensionality of the dot.  $l_0 = \sqrt{\hbar / (m_e \Omega)}$  is the oscillator length corresponding to the modified frequency  $\Omega$  (to be discussed below). The single-particle electron and hole energies in a harmonic oscillator potential and a magnetic field are given by:

$$t_n^{(e)} = \hbar\Omega (2k + |l| + 1) + \hbar\omega_c l / 2, \quad (A2)$$

$$t_n^{(h)} = \frac{m_e}{m_h} \{ \hbar\Omega (2k + |l| + 1) - \hbar\omega_c l / 2 \}, \quad (A3)$$

where  $\Omega = \sqrt{\omega^2 + \omega_c^2 / 4}$ , and  $\omega_c = eB / m_e$  is the electron cyclotron frequency. It is assumed that the confinement potential for holes is such that its characteristic length is  $l_0$  also.

$n, r, s$ , etc are two-dimensional harmonic oscillator states with characteristic length  $l_0$ . They are specified by the radial quantum number,  $k$ , the orbital quantum number (angular momentum projection over  $B$ ),  $l$ , and the spin projection,  $\sigma$ . Notice that we have not included the Zeeman and Overhauser contributions to the single-particle energies (A2,A3). Notice also that the Coulomb matrix element,  $\langle r, s|1/r|u, v \rangle$  is zero unless the spin projections satisfy:  $\sigma_r = \sigma_u, \sigma_s = \sigma_v$ .

There are four conserved charges commuting with the Hamiltonian, (A1). They are:

$$N_{e\uparrow} = \sum_{n\uparrow} e_n^\dagger e_n, \quad N_{e\downarrow} = \sum_{n\downarrow} e_n^\dagger e_n, \quad (\text{A4})$$

$$N_{h\uparrow} = \sum_{n\uparrow} h_n^\dagger h_n, \quad N_{h\downarrow} = \sum_{n\downarrow} h_n^\dagger h_n, \quad (\text{A5})$$

where the notation means that only spin-up electron states enter the sum in  $N_{e\uparrow}$ , etc.

In the BCS function we shall write, the number of spin-up electrons exactly coincide with the number of spin-down holes, and the number of spin-down electrons with the number of spin-up holes. Let us define  $N_+ = N_{e\uparrow}$ , and  $N_- = N_{e\downarrow}$ . The mean value of the Hamiltonian, Eq. (A1), should be minimized with the constraint that the mean values  $\langle N_+ \rangle$  and  $\langle N_- \rangle$  should be fixed. Mean values are obtained by averaging out with the function:

$$|BCS\rangle = \prod_{r\uparrow} (u_r + v_r e_r^\dagger h_r^\dagger) \prod_{s\downarrow} (u_s + v_s e_s^\dagger h_s^\dagger) |0\rangle, \quad (\text{A6})$$

where  $|0\rangle$  denotes the vacuum state, and the ‘‘conjugate’’ hole state  $\bar{n}$  is defined in terms of the electron state  $n = (k, l, \sigma)$  as  $\bar{n} = (k, -l, -\sigma)$ . The coefficients  $u_r, v_r$ , satisfying the normalization conditions  $u_r^2 + v_r^2 = 1$ , are to be used as variational parameters. Notice that

$$\langle N_+ \rangle = \sum_{n\uparrow} v_n^2, \quad \langle N_- \rangle = \sum_{n\downarrow} v_n^2. \quad (\text{A7})$$

The standard BCS equations (gap equations) are obtained by introducing Lagrange multipliers  $\mu_+, \mu_-$ , which are fixed from the equations (A7), and minimizing the function:

$$F(v) = \langle H - \mu_+ N_+ - \mu_- N_- \rangle, \quad (\text{A8})$$

with respect to the variational parameters  $v_n$ . The mean value of the Hamiltonian is given by:

$$\begin{aligned} \langle H \rangle &= \sum_n \left( t_n^{(e)} + t_{\bar{n}}^{(h)} \right) v_n^2 \\ &+ (\beta + \beta' - 2\beta'')/2 \sum_{n,m} \langle n, m|1/r|n, m \rangle v_n^2 v_m^2 \end{aligned}$$

$$\begin{aligned} &- (\beta + \beta')/2 \sum_{n,m} \langle n, m|1/r|m, n \rangle v_n^2 v_m^2 \\ &- \beta'' \sum_{n,m} \langle n, m|1/r|m, n \rangle v_n v_m u_n u_m. \end{aligned} \quad (\text{A9})$$

Notice the exact cancellation of direct Coulomb interactions in the symmetric case,  $\beta = \beta' = \beta''$ .

A rather nontrivial fact, which helps understanding the Lipkin-Nogami scheme, is that the BCS gap equations can also be interpreted as a search for the optimal linear in  $N_+$  and  $N_-$  approximation to  $H$ . Indeed, let us define  $P = \lambda_0 + \lambda_+ N_+ + \lambda_- N_-$ , and require the minimization of the mean square deviation:

$$G(\lambda) = \langle (H - P)^2 \rangle. \quad (\text{A10})$$

The equation:

$$\partial G / \partial \lambda_0 = \langle H - P \rangle = 0, \quad (\text{A11})$$

is used to fix the  $\lambda_0$  parameter, whereas the equations  $\partial G / \partial \lambda_+ = \partial G / \partial \lambda_- = 0$  prove to be equivalent to the BCS gap equations. They can be written in the form:

$$0 = \langle (H - P) N_+ \rangle, \quad (\text{A12})$$

$$0 = \langle (H - P) N_- \rangle. \quad (\text{A13})$$

The chemical potentials,  $\mu_{\pm}$ , can be identified with the  $\lambda_{\pm}$  parameters in the present case.

In the Lipkin-Nogami method, we make a step forward and look for a quadratic approximation to  $H$ :

$$\begin{aligned} P &= \lambda_0 + \lambda_+ N_+ + \lambda_- N_- + \lambda_{++} N_+^2 \\ &+ \lambda_{+-} N_+ N_- + \lambda_{--} N_-^2. \end{aligned} \quad (\text{A14})$$

Minimization of  $G$  in Eq. (A10) leads, in addition to (A11,A12,A13), to the equations:

$$0 = \langle (H - P) N_+^2 \rangle, \quad (\text{A15})$$

$$0 = \langle (H - P) N_-^2 \rangle, \quad (\text{A16})$$

$$0 = \langle (H - P) N_+ N_- \rangle. \quad (\text{A17})$$

Eqs. (A11,A12,A13,A15,A16,A17) conform a linear system from which we obtain the  $\lambda$  parameters in terms of averages like  $\langle H N_+^2 \rangle$ ,  $\langle N_+^2 \rangle$ , etc. In fact, we need only explicit expressions for  $\lambda_{++}$ ,  $\lambda_{+-}$  and  $\lambda_{--}$ :

$$\lambda_{+-} = \frac{\langle HN_+N_- \rangle - \langle HN_+ \rangle \langle N_- \rangle - \langle N_+ \rangle \langle HN_- \rangle + \langle H \rangle \langle N_+ \rangle \langle N_- \rangle}{\langle N_+^2 \rangle \langle N_-^2 \rangle - \langle N_+^2 \rangle \langle N_- \rangle^2 - \langle N_+ \rangle^2 \langle N_-^2 \rangle + \langle N_+ \rangle^2 \langle N_- \rangle^2}, \quad (\text{A18})$$

$$\lambda_{++} = \frac{(\langle HN_+^2 \rangle - \langle H \rangle \langle N_+^2 \rangle)(\langle N_+^2 \rangle - \langle N_+ \rangle^2) - (\langle HN_+ \rangle - \langle H \rangle \langle N_+ \rangle)(\langle N_+^3 \rangle - \langle N_+ \rangle \langle N_+^2 \rangle)}{(\langle N_+^4 \rangle - \langle N_+^2 \rangle^2)(\langle N_+^2 \rangle - \langle N_+ \rangle^2) - (\langle N_+^3 \rangle - \langle N_+ \rangle \langle N_+^2 \rangle)^2}, \quad (\text{A19})$$

and similarly for  $\lambda_{--}$ . The parameters  $\lambda_+$  and  $\lambda_-$  are absorbed into the definition of the chemical potentials:

$$\mu_+ = \lambda_+ + 2\lambda_{++}\langle N_+ \rangle + \lambda_{+-}\langle N_- \rangle, \quad (\text{A20})$$

(and similarly for  $\mu_-$ ). They are obtained from Eqs. (A7), in which we introduce the standard parametrization:

$$v_{n\uparrow}^2 = \frac{1}{2} \left( 1 - \frac{\varepsilon_{n\uparrow}^{HF} - \mu_+}{\sqrt{(\varepsilon_{n\uparrow}^{HF} - \mu_+)^2 + (\Delta_n^+)^2}} \right), \quad (\text{A21})$$

and similarly for  $v_{n\downarrow}^2$ . The pair Hartree-Fock energy is given by:

$$\begin{aligned} \varepsilon_{n\uparrow}^{HF} &= t_n^{(e)} + t_{\bar{n}}^{(h)} - \beta'' \langle n, n | 1/r | n, n \rangle - \lambda_{++}(u_n^2 - v_n^2) \\ &+ (\beta + \beta' - 2\beta'') \sum_{k\uparrow \neq n\uparrow} \langle n, k | 1/r | n, k \rangle v_k^2 \\ &+ (\beta + \beta' - 2\beta'') \sum_{k\downarrow} \langle n, k | 1/r | n, k \rangle v_k^2 \\ &- (\beta + \beta') \sum_{k\uparrow \neq n\uparrow} \langle n, k | 1/r | k, n \rangle v_k^2. \end{aligned} \quad (\text{A22})$$

The gap parameters,  $\Delta_n^+$ , introduced in Eq. (A21), are obtained from Eq. (A12). The latter can be put in the form of gap equations:

$$\begin{aligned} \langle N_+^4 \rangle &= \langle N_+ \rangle^4 + 6\langle N_+ \rangle^3 + 7\langle N_+ \rangle^2 + \langle N_+ - (6\langle N_+ \rangle^2 + 18\langle N_+ \rangle + 7) \sum_{n\uparrow} v_n^4 \\ &+ 4(2\langle N_+ \rangle + 3) \sum_{n\uparrow} v_n^6 + 3 \left( \sum_{n\uparrow} v_n^4 \right)^2 - 6 \sum_{n\uparrow} v_n^8, \end{aligned} \quad (\text{A26})$$

and similarly for  $\langle N_-^2 \rangle$ , etc. Notice that, because of the factorizable form Eq. (A6), mean values like  $\langle N_+N_- \rangle$

$$\langle HN_+ \rangle = \langle H \rangle \langle N_+ \rangle + \sum_{n\uparrow} \left( t_n^{(e)} + t_{\bar{n}}^{(h)} \right) v_n^2 u_n^2$$

$$\Delta_n^+ = \beta'' \sum_{s\uparrow} \langle n, s | 1/r | s, n \rangle \frac{\Delta_s^+}{\sqrt{(\varepsilon_s^{HF} - \mu_+)^2 + (\Delta_s^+)^2}}, \quad (\text{A23})$$

and similarly for  $\Delta_n^-$ .

The iterative procedure designed to solve these equations is as follows. We start from a set  $\{\varepsilon_n^{(HF)}, \Delta_n\}$ . Eqs. (A21) are introduced into Eqs. (A7) and the chemical potentials  $\mu_+, \mu_-$  are found. Then, we compute  $\lambda_{++}, \lambda_{+-}$  and  $\lambda_{--}$ . Hartree-Fock energies and gap functions are recalculated from Eqs. (A22,A23), and the process is repeated until convergence is reached.

For completeness, let us write the explicit expressions for the mean values needed to compute  $\lambda_{++}, \lambda_{+-}$  and  $\lambda_{--}$ :

$$\begin{aligned} \langle N_+^2 \rangle &= \sum_{n\uparrow, m\uparrow} \{v_n^2 v_m^2 + \delta_{nm} v_n^2 u_n^2\} \\ &= \langle N_+ \rangle^2 + \langle N_+ \rangle - \sum_{n\uparrow} v_n^4, \end{aligned} \quad (\text{A24})$$

$$\begin{aligned} \langle N_+^3 \rangle &= \langle N_+ \rangle^3 + 3\langle N_+ \rangle^2 + \langle N_+ \rangle \\ &- 3(\langle N_+ \rangle + 1) \sum_{n\uparrow} v_n^4 + 2 \sum_{n\uparrow} v_n^6, \end{aligned} \quad (\text{A25})$$

factorize,  $\langle N_+N_- \rangle = \langle N_+ \rangle \langle N_- \rangle$ . Concerning mean values of  $H$  with powers of  $N_+$ , we have:

$$\begin{aligned}
& + \sum_{n\uparrow, m} \{(\beta + \beta' - 2\beta'')\langle n, m|1/r|n, m\rangle - (\beta + \beta')\langle n, m|1/r|m, n\rangle\} v_n^2 v_m^2 (1 - v_n^2) \\
& - \beta'' \sum_{n\uparrow, m\uparrow} \langle n, m|1/r|m, n\rangle v_n u_n v_m u_m (1 - 2v_n^2),
\end{aligned} \tag{A27}$$

$$\begin{aligned}
\langle HN_+ N_- \rangle & = \langle HN_+ \rangle \langle N_- \rangle + \langle HN_- \rangle \langle N_+ \rangle - \langle H \rangle \langle N_+ \rangle \langle N_- \rangle \\
& + (\beta + \beta' - 2\beta'') \sum_{n\uparrow, m\downarrow} \langle n, m|1/r|n, m\rangle v_n^2 u_n^2 v_m^2 u_m^2,
\end{aligned} \tag{A28}$$

$$\begin{aligned}
\langle HN_+^2 \rangle & = \langle H \rangle \langle N_+^2 \rangle + 2\langle N_+ \rangle (\langle HN_+ \rangle - \langle H \rangle \langle N_+ \rangle) + \sum_{n\uparrow} (t_n^{(e)} + t_n^{(h)}) u_n^2 v_n^2 (1 - 2v_n^2) \\
& + (\beta + \beta' - 2\beta'') \sum_{n\uparrow, m} \langle n, m|1/r|n, m\rangle v_n^2 v_m^2 u_n^2 (u_n^2 - v_n^2) \\
& + (\beta + \beta' - 2\beta'') \sum_{n\uparrow, m\uparrow} \langle n, m|1/r|n, m\rangle v_n^2 v_m^2 u_n^2 u_m^2 \\
& - (\beta + \beta') \sum_{n\uparrow, m\uparrow} \langle n, m|1/r|m, n\rangle (2v_n^2 v_m^2 - 5v_n^4 v_m^2 + 2v_n^6 v_m^2 + v_n^4 v_m^4) \\
& - \beta'' \sum_{n\uparrow, m\uparrow} \langle n, m|1/r|m, n\rangle v_n u_n v_m u_m (1 - 6v_n^2 + 4v_n^4 + 2v_n^2 v_m^2).
\end{aligned} \tag{A29}$$

Notice that, from Eq. (A28) it follows that  $\lambda_{+-} = 0$  in the symmetric system with  $\beta = \beta' = \beta''$ . Finally, the Lipkin-Nogami energy is obtained by replacing the operators  $N_+$ ,  $N_-$  in  $P$  by its eigenvalues. It can be written in the form:

$$\begin{aligned}
E_{LN} & = \langle H \rangle - \lambda_{++} (\langle N_+^2 \rangle - \langle N_+ \rangle^2) \\
& - \lambda_{--} (\langle N_-^2 \rangle - \langle N_- \rangle^2).
\end{aligned} \tag{A30}$$

To get an idea of the intensities of the luminescence

lines, we compute the matrix elements of the interband dipole operator:

$$D_+ = \sum_{n\uparrow} e_n h_{\bar{n}}. \tag{A31}$$

A similar expression can be written for  $D_-$ . The intensity of the transition from the ground state of the  $(N_+, N_-)$  system to the ground state of the  $(N_+ - 1, N_-)$  system is proportional to the matrix element of  $D_+$  squared:

$$I_+ = |\langle N_+ - 1, N_- | D_+ | N_+, N_- \rangle|^2 = \left| \prod_{n\downarrow} (u'_n u_n + v'_n v_n) \right|^2 \left| \sum_{n\uparrow} u'_n v_n \prod_{j\uparrow \neq n\uparrow} (u'_j u_j + v'_j v_j) \right|^2, \tag{A32}$$

where  $(u, v)$  and  $(u', v')$  are, respectively, the BCS coefficients for the initial and final states. It can be verified that the transition from the ground state of the  $(N_+, N_-)$  system to the ground state of the  $(N_+ - 1, N_-)$  system accounts for most of the transition probability. Indeed, a total intensity can be defined in the following way:

$$I_+^{total} = \sum_{\psi} |\langle \psi | D_+ | N_+, N_- \rangle|^2$$

$$= \sum_{n\uparrow} v_n^4 + \left( \sum_{n\uparrow} u_n v_n \right)^2, \tag{A33}$$

where the sum runs over all possible final states,  $|\psi\rangle$ . For the (2,1) complex at  $B = 1$  Tesla, with the parameters used in this paper,  $I_+/I_+^{total} = 0.84$ , whereas for the (10,9) system,  $I_+/I_+^{total} = 0.92$ .

The two terms in Eq. (A33) have a simple interpretation. If pairing is neglected, the decay of a pair in the state  $n$  proceeds independently of the rest of the states.



The matrix element of  $D_+$  is equal to the probability of finding a pair in the state  $n$ , i.e., to  $v_n^2$ . Thus,  $D_+$  squared equals  $v_n^4$ . The first term in Eq. (A33) is hence the probability of decay of individual pairs. The sec-

ond term comes from pairing. In our model, at  $B = 1$  Tesla,  $I_+^{total}$  from the (7,6) complex, for example, has a component coming from individual decays equal to 5.20, whereas the pairing contribution reaches the value 59.34.

- 
- <sup>1</sup> S. P. Najda, S. Takeyama, N. Miura et. al., Phys. Rev. B **40**, 6189 (1989); M.J. Snelling, G. P. Flinn, A.S. Plaut, R. T. Harley, A. C. Tropper, R. Eccleston, and C. C. Phillips, Phys. Rev. B **44**, 11345 (1991); M. J. Snelling, E. Blackwood, C. J. McDonagh, R. T. Harley, and C. T. B. Foxon, Phys. Rev. B **45**, 3922 (1992); N. J. Traynor, R. J. Warburton, M. J. Snelling, and R. T. Harley, Phys. Rev. B **55**, 15701 (1997); M. Seck, M. Potemski, and P. Wyder, Phys. Rev. B **56**, 7422 (1997).
- <sup>2</sup> D. Paget, G. Lampel, B. Sapoval, and V.I. Safarov, Phys. Rev. B **15**, 5780 (1977).
- <sup>3</sup> D. Gammon, A.L. Efros, T.A. Kennedy, M. Rosen, D.S. Katzer, D. Park, S.W. Brown, V.L. Korenev, and I.A. Merkulov, Phys. Rev. Lett. **86**, 5176 (2001).
- <sup>4</sup> T. Yokoi, S. Adachi, H. Sasakura, S. Muto, H.Z. Song, T. Uzuki, and S. Hirose, <http://arxiv.org/abs/cond-mat/0407227>.
- <sup>5</sup> S.W. Brown, T.A. Kennedy, D. Gammon, and E.S. Snow, Phys. Rev. B **54**, R17339 (1996).
- <sup>6</sup> A.A. Radzig and B.M. Smirnov, Manual of atomic and molecular physics, Atomizdat, Moscow, 1980 (in russian).
- <sup>7</sup> D. Paget, G. Lampel, B. Sapoval, and V.I. Safarov, Phys. Rev. B **15**, 5780 (1977).
- <sup>8</sup> D. Gammon, E.S. Snow, B.V. Shanabrook, D.S. Katzer, and D. Park, Phys. Rev. Lett. **76**, 3005 (1996).
- <sup>9</sup> D. Gammon, S.W. Brown, E.S. Snow, T.A. Kennedy, D.S. Katzer, and D. Park, Science **277**, 85 (1997); S.W. Brown, T.A. Kennedy, and D. Gammon, Solid. State Nuclear Magnetic Resonance **11**, 49 (1998).
- <sup>10</sup> J. Dobaczewski and W. Nozarewickz, Phys. Rev C **47**, 2418 (1993), and references cited therein.
- <sup>11</sup> B.A. Rodriguez and A. Gonzalez, Phys. Rev. B **63**, 205324 (2001).
- <sup>12</sup> R. Perez and A. Gonzalez. Physica **E 8** (2000) 91.
- <sup>13</sup> E. Dekel, D. Gershoni, E. Ehrenfreund, D. Spektor, J.M. Garcia, and P.M. Petrof, Phys. Rev. Lett. **80**, 4991 (1998).